

Probing flavored regimes of leptogenesis with gravitational waves from cosmic strings

Marco Chianese,^{1, 2, a} Satyabrata Datta,^{3, b} Gennaro Miele,^{1, 2, 4, c} Rome Samanta,^{4, 2, d} and Ninetta Saviano^{2, 4, e}

¹*Dipartimento di Fisica “Ettore Pancini”, Università degli studi di Napoli “Federico II”,
Complesso Univ. Monte S. Angelo, I-80126 Napoli, Italy*

²*INFN - Sezione di Napoli, Complesso Univ. Monte S. Angelo,
I-80126 Napoli, Italy* ³*Scuola Superiore Meridionale,
Università degli studi di Napoli “Federico II”, Largo San Marcellino 10, 80138 Napoli, Italy*

³*Department of Physics and Institute of Theoretical Physics,
Nanjing Normal University, Nanjing, 210023, China*

⁴*Scuola Superiore Meridionale, Largo S. Marcellino 10, I-80138 Napoli, Italy*

Cosmic strings radiate detectable gravitational waves in models featuring high-scale symmetry breaking, e.g., high-scale leptogenesis. In this Letter, for the first time, we show that different flavored regimes of high-scale leptogenesis can be tested distinctly with the spectral features in cosmic string-radiated gravitational waves. This is possible if the scalar field that makes right-handed neutrinos massive is feebly coupled to the Standard Model Higgs. Each flavored regime, sensitive to low-energy neutrino experiments, leaves a marked imprint on the gravitational waves spectrum. A three-flavor and a two-flavor regime could be probed by a characteristic fall-off of the gravitational wave spectrum at the LISA-DECIGO-ET frequency bands with preceding scale-invariant amplitudes bounded from above and below. We present Gravitational Waves windows for Flavored Regimes of Leptogenesis (GWFL) falsifiable in the upcoming experiments.

Introduction. Within the framework of the seesaw mechanism of light neutrino masses, leptogenesis [1] is a simple process for obtaining the observed baryon asymmetry of the universe [2]. In this process, CP asymmetric and out-of-equilibrium decays of heavy right-handed neutrinos (RHNs) to lepton and the Standard Model (SM) Higgs doublets, create a lepton asymmetry, which is then processed to baryon asymmetry by sphalerons [3]. In the thermal leptogenesis scenario, the lepton asymmetry gets produced at a temperature $T_{\text{lepto}} \sim M_N$, where M_N is the mass of the decaying RHN – also referred to as the scale of thermal leptogenesis [4, 5]. Despite being a simple mechanism, leptogenesis operating on scales $M_N > \mathcal{O}(\text{TeV})$ are not directly testable, e.g., with collider experiments. Accurate incorporation of flavor effects [6–8] nonetheless opens up the opportunity to test high-scale leptogenesis with low-energy neutrino observables, specifically with the leptonic CP violation [9] – a measurement of which is one of the primary goals of the ongoing neutrino experiments such as T2K [10] and NO ν A [11]. Depending on the interaction strengths of the charged lepton flavors, there exist three distinct regimes of high-scale leptogenesis: $M_N \gtrsim 10^{12}$ GeV (one-flavor/vanilla, 1FL), 10^9 GeV $\lesssim M_N \lesssim 10^{12}$ GeV (two-flavor, 2FL), and $M_N \lesssim 10^9$ GeV (three-flavor, 3FL). While the 1FL regime is not sensitive to neutrino mixing parameters, the 2FL and 3FL regimes can offer low-energy neutrino phenomenology, which however may not be unequivocal, because of plenty of free parameters in

the seesaw Lagrangian. Lately, there have been efforts to obtain a direct possible signature of high-scale leptogenesis with primordial stochastic gravitational waves background (SGWB) by focusing on the RHN sector, specifically, on the leptogenesis scale. This is interesting and wholesome because, unlike electromagnetic radiation, GWs traverse the early universe unimpeded with unerring information about their origin. Therefore, no matter how high the leptogenesis scale is, it can be probed with GWs. The idea originates from contemplating the origin of RHN mass at a more fundamental level [12–15]. In Ref. [12] it has been argued that the RHNs become massive because of the spontaneous breaking of a $U(1)_{B-L}$ gauge invariance, which many Grand Unified Theories (GUT) naturally embed [16–19]. Besides generating RHN mass, a gauged $U(1)_{B-L}$ breaking inevitably produces cosmic strings that radiate gravitational waves, which may be a signature of leptogenesis. Let us consider the $U(1)_{B-L}$ invariant RHN mass term $f_N \bar{N}_R \Phi N_R^C$, where f_N is the Yukawa coupling, N_R is the RHN field and Φ being the $B-L$ scalar with vacuum expectation value v_Φ . After the $U(1)_{B-L}$ breaking, the RHNs obtain mass given by $M_N = f_N v_\Phi$, cosmic strings are formed [20–22] and radiate GWs with a scale-invariant spectrum at higher frequencies with an overall amplitude $\Omega_{GW} \propto v_\Phi$ [23, 24]. While the scenario is interesting, note however, that the GW spectrum being dependent only on v_Φ is not so sensitive to M_N because of the additional free parameter f_N . As such, a GW spectrum for $v_\Phi = 10^{14}$ GeV may correspond to 3FL for $f_N = 10^{-6}$ as well as 2FL for $f_N = 10^{-4}$. Therefore, a more realistic GW signature of leptogenesis requires dependence on both parameters v_Φ and f_N , hence on M_N .

In this Letter, we show that the M_N -dependent GW spectrum and a concrete link between GWs and high-scale leptogenesis can be achieved in the context of

^a marco.chianese@unina.it

^b amisatyabrata703@gmail.com

^c miele@na.infn.it

^d samanta@na.infn.it

^e nsaviano@na.infn.it

$U(1)_{B-L}$ model with a peculiar scalar field dynamics [25]. After the phase transition, Φ rolls down to its true vacuum and oscillates coherently to provide an early matter-domination when it is long-lived. If the lifetime of the scalar field gets determined by v_Φ and f_N , then M_N regulates the beginning and the end of the matter-domination. Differently from Ref. [12], the amplitude and the spectral features of the GWs radiated from cosmic strings are imprinted by the M_N -dependent matter domination, thus carrying information on M_N , and therefore, different regimes of flavored leptogenesis. In particular, the scale invariance in the GW spectrum at higher frequencies breaks at a frequency f_{dec} determined by the end of the matter domination at the temperature $T_{\text{dec}}(M_N)$ (see Fig. 1). We point out that such a scenario allows us to probe the RHN mass scale markedly, in agreement with all the relevant constraints on the parameter space (see Fig. 2): *i*) the bound from the recent observations of nHz GWs by Pulsar Timing Arrays (PTA) [26–30] which disfavor GWs from cosmic strings [31]; *ii*) the condition that the cosmic strings radiate predominantly GWs than particles [32, 33]; *iii*) the requirement that the Φ decays before the Big-Bang-Nucleosynthesis (BBN) [34, 35]. We highlight that if the break of the GW spectrum occurs in the LISA (ET) frequency band, most likely it is a signature of a 3FL (2FL) regime. Remarkably, the amplitudes and the spectral break frequencies of the GW spectra predicted by our model are very well delimited and they are all within reach of planned gravitational wave experiments such as LISA, DECIGO and ET [36–38]. This ensures unique and highly testable GW signatures of flavor regimes of high-scale leptogenesis.

The parameter space for M_N -dependent matter domination. The seesaw Lagrangian for neutrino masses and leptogenesis is given by

$$-\Delta\mathcal{L} \subset f_{Di\alpha}\overline{N_{Ri}}\tilde{H}^\dagger L_\alpha + \frac{1}{2}f_{Ni}\overline{N_{Ri}}\Phi N_{Ri}^C + \text{h.c.}, \quad (1)$$

where f_D is the neutrino Dirac Yukawa coupling and $H(L)$ is the SM Higgs (lepton doublet). The fields N_R and L have $B-L$ charge -1 , whereas the same charges for Φ and H are 2 and 0 , respectively. The scalar field dynamics is dictated by the finite temperature potential restoring symmetry at higher temperatures given by [39, 40]

$$V(\Phi, T) = \frac{\lambda}{4}\Phi^4 + D(T^2 - T_0^2)\Phi^2 - ET\Phi^3, \quad (2)$$

where D, E and T_0 are functions of $B-L$ gauge coupling g' , λ is the self-interaction coupling, and the zero temperature potential $V(\Phi, 0) = -\frac{\mu^2}{2}\Phi^2 + \frac{\lambda}{4}\Phi^4$ determines the vacuum expectation value $v_\Phi = \mu/\sqrt{\lambda}$. The last term in Eq. (2) generates a potential barrier causing a secondary minimum at $\Phi \neq 0$, which becomes degenerate with the $\Phi = 0$ one at $T = T_c$. The potential barrier vanishes at T_0 ($\lesssim T_c$), and the minimum at $\Phi = 0$ becomes a maximum. The transition from $\Phi = 0$ to $\Phi = v_\Phi$ can be

treated as a second-order transition with an extremely quick disappearance of the potential barrier if the order parameter $\Phi_c/T_c \ll 1$ (weakly first-order transition). Such a smooth transition can be obtained approximately within the ballpark of $\lambda \simeq g'^3$ and for $g' \lesssim 10^{-2}$ [13, 41]. Once Φ rolls down, it oscillates around v_Φ behaving as matter [25, 42, 43]. Three important observations are in order. First, the $U(1)_{B-L}$ breaking scale can be as high as the GUT scale, implying $v_\Phi \lesssim 5 \times 10^{15}$ GeV. Second, the Hubble friction at T_c should also be negligible for the rolling of the field down to v_Φ ; this can be achieved by considering m_Φ larger than the Hubble parameter $\mathcal{H}(T_c)$. Third, RHNs become massive after the phase transition at $T = T_c$. Therefore, the scale of leptogenesis $T_{\text{lepto}} \sim M_N$ is bounded from above as $T_{\text{lepto}} \sim M_N \lesssim T_c$.

We aim to make Φ long-lived to induce a matter-domination epoch with a lifetime determined by v_Φ and f_N . In high-scale leptogenesis scenario, the coupling f_N should be generically large to have M_N comparable with v_Φ . In such a case, if $m_\Phi > 2M_N$, tree-level decay of Φ to RHN pairs ($\Phi \rightarrow NN$) would be too quick to make Φ long-lived. This restricts ourselves to the case $M_N > m_\Phi = \sqrt{2\lambda}v_\Phi$. Therefore, along with $M_N \lesssim T_c$, the Φ scalar is long-lived within the following range

$$\sqrt{2g'}g'v_\Phi < M_N \lesssim 2\sqrt{g'}v_\Phi, \quad (3)$$

where we have assumed $\lambda = g'^3$. In this case, the mass of Φ is suppressed by a factor $\sqrt{g'}$ compared to the $M_{Z'} = \sqrt{2g'}v_\Phi$, thus kinematically forbidding the tree-level decays of Φ to Z' pairs. Note interestingly that the seesaw Lagrangian in Eq. (1) can provide an effective coupling $\lambda_{\Phi H, 1\text{-loop}} \sim f_D^2 f_N^2 / (2\pi^2)$ at one-loop to trigger $\Phi \rightarrow HH$ decay. Therefore, despite f_N being large, we can have a smaller decay rate as it is proportional to $\lambda_{\Phi H, 1\text{-loop}}^2$. This decay involves both: the RHN mass and the active neutrino mass m_ν via the Dirac Yukawa coupling $f_D = \sqrt{m_\nu} f_N v_\Phi / v_H^2$. In our discussion, we shall consider this radiative $\Phi \rightarrow HH$ decay with the assumption that $\lambda_{\Phi H, 1\text{-loop}} \gg \lambda_{\Phi H, \text{tree}}$. The decay rate up to a logarithmic factor is given by [25, 44, 45]

$$\Gamma_\Phi^{HH} \simeq \Gamma_0 \left(\frac{g'}{10^{-5}} \right)^3 \left(\frac{v_\Phi}{10^{13} \text{ GeV}} \right)^2 \left(\frac{m_\Phi}{10^8 \text{ GeV}} \right), \quad (4)$$

with $\Gamma_0 = 1.3 \times 10^{-17}$ GeV. We have assumed $m_\nu \simeq 0.01$ eV, the SM Higgs vacuum expectation value $v_H = 174$ GeV, and $f_N \simeq g' \ll 1$, which implies $M_N \simeq M_{Z'} \ll v_\Phi$. The latter assumption should not drastically change the phenomenological implication of the scenario because of the constraint in Eq. (3).

The evolution of the energy density of Φ and the duration of matter domination epoch, which ends when Φ decay [25], can be tracked by solving the Friedman equations (see Supplemental Material I for further details). The decay temperature of the scalar field can be obtained

analytically considering $\Gamma_{\Phi}^{HH} \simeq \mathcal{H}$, and is given by

$$T_{\text{dec}} \simeq 6.35 \left(\frac{g'}{10^{-5}} \right)^{3/4} \left(\frac{M_N}{10^9 \text{ GeV}} \right)^{3/2} \text{ GeV}, \quad (5)$$

where we consider $M_N = g'v_{\Phi}$. The scalar decays must occur before BBN, i.e., $T_{\text{dec}} \gtrsim T_{\text{BBN}} \sim 10 \text{ MeV}$. Moreover, because the scalar field is long-lived, it produces entropy which dilutes any pre-existing relic, including the baryon asymmetry. The amount of entropy production in our scenario can be computed as $\kappa \simeq 140(g'/10^{-3})^{-1/4}(M_N/10^9 \text{ GeV})^{-1/2}$. The entropy dilution by a factor of κ^{-1} must be considered in the computation of baryon asymmetry. Even in the low M_N region, the scenario does not allow large entropy dilution [25], consequently the baryon asymmetry can be comfortably generated. Finally, we mention that we can safely neglect the additional one-loop decay $\Phi \rightarrow f\bar{f}V$ (the two-body decay $\Phi \rightarrow f\bar{f}$ is suppressed due to chirality flip [46]), where f and V are SM fermions and vector bosons. Indeed, this decay dominates over the $\Phi \rightarrow HH$ only for $g' \gtrsim 10^{-2}$ and smaller values of v_{Φ} , which is outside our parameter space.

Imprints of flavored leptogenesis on GWs from cosmic string. Gravitational waves are radiated from cosmic string loops chopped off from the long strings resulting from the spontaneous breaking of the gauged $U(1)_{B-L}$ [23, 24]. Long strings are described by a correlation length $L = \sqrt{\mu/\rho_{\infty}}$, with ρ_{∞} is the long string energy density and μ is the string tension defined as [47]

$$\mu = \pi v_{\Phi}^2 h(\lambda, g') \quad \text{with} \quad h \simeq \frac{1}{\ln(2g'^2/\lambda)}, \quad (6)$$

for $\lambda \ll 2g'^2$. In the present analysis, we take $\lambda = g'^3$ therefore $h \simeq 1/\ln(2/g')$. The time evolution of a radiating loop of initial size $l_i = \alpha t_i$ is given by $l(t) = l_i - \Gamma G\mu(t - t_i)$, where $\Gamma \simeq 50$ [23, 24], $\alpha \simeq 0.1$ [48, 49], $G = M_{\text{Pl}}^{-2}$, and t_i being the initial time of loop creation. The total energy loss from a loop is decomposed into a set of normal-mode oscillations with frequencies $f_k = 2k/l_k = a(t_0)/a(t)f$, where $k = 1, 2, 3, \dots, k_{\text{max}}$, f is the present-day frequency at t_0 , and a is the scale factor. The total GW energy density is computed by summing all the k modes giving [48, 49]

$$\Omega_{GW}(f) = \sum_{k=1}^{k_{\text{max}}} \frac{2k\mathcal{F}_{\alpha}G\mu^2\Gamma_k}{f\rho_c} \int_{t_i}^{t_0} \left[\frac{a(t)}{a(t_0)} \right]^5 n_{\omega}(t, l_k) dt, \quad (7)$$

where ρ_c is the critical energy density of the universe, $\mathcal{F}_{\alpha} \simeq 0.1$ is an efficiency factor [48] and $n_{\omega}(t, l_k)$ is the loop number density. The latter can be computed from the velocity-dependent-one-scale model as [50–53]

$$n_{\omega}(t, l_k) = \frac{A_{\beta}}{\alpha} \frac{(\alpha + \Gamma G\mu)^{3(1-\beta)}}{[l_k(t) + \Gamma G\mu t]^{4-3\beta} t^{3\beta}}, \quad (8)$$

where $\beta = 2/3(1 + \omega)$ with ω being the equation of state parameter of the universe, and $A_{\beta} = 5.4$ ($A_{\beta} = 0.39$) for

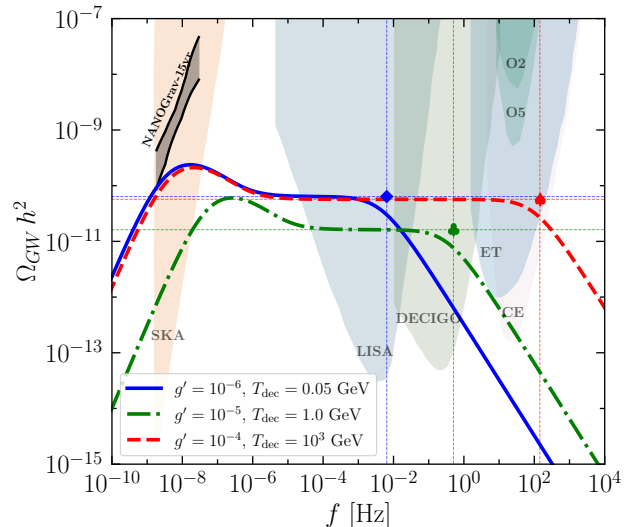


FIG. 1. The GW spectrum from cosmic string as predicted by our model for three benchmark choices for the parameter g' and T_{dec} , with M_N uniquely fixed by Eq. (5) (see text for details). Blue and green spectra correspond to 3FL, while the red one is for 2FL. The symbols show the analytical calculations of the GW plateau amplitude and the break frequency according to Eq.s (9) and (10), respectively.

radiation-dominated (matter-dominated) universe [53]. The quantity $\Gamma_k = \Gamma k^{-\delta}/\zeta(\delta)$ quantifies the emitted power in k -th mode, with $\delta = 4/3$ ($\delta = 5/3$) for loops containing cusps (kinks) [54]. We shall present the results for the dominant $k = 1$ mode which captures the qualitative features of our analysis.

The integral in Eq. (7) is subjected to two Heaviside functions $\Theta(t_i - t_{\text{fric}})\Theta(t_i - l_c/\alpha)$ which set cut-offs on the GW spectrum at very high frequencies f_* above which it falls as f^{-1} . The quantity t_{fric} represents the time until which the motion of the string network is damped by friction [55], and l_c is a critical length above which GW emission is dominant over particle production as shown by high-resolution numerical simulations [32, 33]. The critical length is $l_c \simeq \delta_w(\Gamma G\mu)^{-\gamma}$ where $\delta_w = (\sqrt{\lambda}v_{\Phi})^{-1}$ is the width of the string and $\gamma = 2$ ($\gamma = 1$) for loops containing cusps (kinks). Note that we deal with small values of λ leading to “fat” strings, which are not conventional while studying GWs signatures from cosmic strings in BSM models [12]. In particular, in this case, the particle production cut-off in the GW spectrum is much stronger than the one usually considered for “thin strings” ($\lambda \simeq 1$). Thus, our scenario is also the first concrete BSM model that discusses the results of [32, 33] for small λ .

In Fig. 1, we show the GW spectrum from Eq. (7) (for $k = 1$) predicted by our model for three benchmark scenarios: $g' = 10^{-6}$ and $T_{\text{dec}} = 0.05 \text{ GeV}$ (blue line), $g' = 10^{-5}$ and $T_{\text{dec}} = 1 \text{ GeV}$ (green line), $g' = 10^{-4}$ and $T_{\text{dec}} = 10^3 \text{ GeV}$ (red line), with the scale M_N of leptoge-

nesis being uniquely defined by Eq. (5) to be 1.3×10^8 , 2.9×10^8 and 9.2×10^9 in units of GeV, respectively. Without any intermediate matter-dominated epoch, the GW spectrum has two main contributions: a low-frequency peak owing to the GW radiation from the loops which are created in the radiation epoch and decay in the standard matter epoch, and an almost scale-invariant plateau at high frequencies as [48, 49, 56]

$$\Omega_{GW}^{\text{plt}}(f) = \frac{128\pi\mathcal{F}_\alpha G\mu}{9\zeta(\delta)} \frac{A_R}{\epsilon_R} \Omega_R \left[(1 + \epsilon_R)^{3/2} - 1 \right], \quad (9)$$

that arises from loop creation and decay in the radiation-dominated epoch only. In Eq. (9), $\epsilon_R = \alpha/\Gamma G\mu \gg 1$, $A_R \equiv A_\beta \simeq 5.4$ and $\Omega_R \sim 9 \times 10^{-5}$. Note that $\Omega_{GW}^{\text{plt}}(f) \propto \sqrt{\mu} \propto v_\Phi$, implying, the larger the symmetry breaking scale, the stronger the amplitude of GW. In our scenario, which features instead an intermediate matter-dominated epoch, the plateau breaks at a high frequency f_{dec} , beyond which the spectrum falls as $\Omega_{GW}(f > f_{\text{dec}}) \sim f^{-1}$ (see Fig. 1). The analytical expression for this spectral break frequency f_{dec} can be computed as [57]

$$f_{\text{dec}} \simeq \sqrt{\frac{8z_{\text{eq}}}{\alpha\Gamma G\mu}} \left(\frac{t_{\text{eq}}}{t_{\text{dec}}} \right)^{1/2} t_0^{-1}, \quad (10)$$

where $z_{\text{eq}} \simeq 3400$ is the red-shift at the standard matter-radiation equality taking place at time t_{eq} , while t_{dec} is the time at which the scalar field Φ decays (matter domination ends). For the three benchmark cases in Fig. 1, the break of the GW spectrum occurs in the LISA [36], DECIGO [37] and ET [38] frequency bands, respectively.

In order to robustly claim the spectral fall as a signature of M_N -dependent matter domination, we must require both $t_{\text{dec}} > l_c/\alpha$ and $t_{\text{dec}} > t_{\text{fric}}$. The first condition leads to the constraint

$$M_N \gtrsim M_N^c \left(\frac{T_{\text{dec}}}{\text{GeV}} \right)^{2/5} \left(\frac{g'}{10^{-5}} \right)^{7/10} h(g')^{-2/5}, \quad (11)$$

with $M_N^c = 3.8 \times 10^7$ GeV. Similar constraints can be derived for loops containing kinks, which however are less stringent. The second condition $t_{\text{dec}} > t_{\text{fric}}$ implies

$$M_N \gtrsim M_N^{\text{fric}} \left(\frac{T_{\text{dec}}}{\text{GeV}} \right)^{1/2} \left(\frac{g'}{10^{-5}} \right) h(g')^{-1/2}, \quad (12)$$

with $M_N^{\text{fric}} = 2.0 \times 10^4$ GeV.

The parameter space of our model is also constrained by the recent PTA observations of stochastic GW which disfavor cosmic strings due to a different spectral slope [31]. Thus, PTA data require $\Omega_{GW} < \Omega_{GW}^{\text{PTA}}$ at $f = 30$ nHz giving $G\mu \lesssim 7.0 \times 10^{-11}$. This translates to the constraint on M_N as

$$M_N \lesssim M_N^{\text{PTA}} \left(\frac{g'}{10^{-5}} \right) h(g')^{-1/2}, \quad (13)$$

whit $M_N^{\text{PTA}} \simeq 5.6 \times 10^8$ GeV. All these constrained are satisfied by the benchmark cases shown in Fig. 1.

We note that there could be additional contribution to the GW spectrum at very high frequencies due to the cosmic string loops in the first radiation epoch before Φ starts to dominate. However, the amplitude at higher frequencies is suppressed not only because of the entropy production, but also because the hard particle production cut-off makes the spectrum red.

Results and discussion. In Fig. 2, we show the sensitivities of LISA, DECIGO and ET in the plane $T_{\text{dec}}-M_N$, assuming $g' = 10^{-6}$ (left panel), $g' = 10^{-5}$ (middle panel) and $g' = 10^{-4}$ (right panel), together with all the conditions and constraints discussed above. We underline that the dependence of the GW sensitivities on g' comes from the relation $M_N = (G\mu g'^2 M_{\text{Pl}}^2/\pi/h(g'))^{1/2}$. The white regions in each plot can be generally regarded as allowed parameter space when taking T_{dec} and M_N as independent parameters. However, in our model, they are related by Eq. (5) which restricts the allowed parameter space along the solid colored lines in the plots. Overall, the requirement of negligible particle production from cosmic string, the recent PTA data, and the BBN constraint limit the parameter space to be $g' \sim [10^{-6}, 10^{-4}]$ and $M_N/\text{GeV} \sim [10^7, 10^{10}]$.

We find that, irrespective of the values of g' , going from light to heavy M_N region along the colored lines, the spectral break frequency f_{dec} increases according to Eq.s (5) and (10). This trend allows us to point out that if the spectral break occurs in the LISA band, it most likely corresponds to $M_N \lesssim 10^9$ (3FL regime), as proven by the allowed segment of the blue line in the left plot. With a similar argument, a spectral break in the ET band would correspond to a 2FL regime of leptogenesis, as depicted by the red line in the right plot. An intermediate situation with $g' = 10^{-5}$, both the 2FL and 3FL regions would provide a spectral break in the DECIGO frequency band. Therefore, in this frequency band, the spectral break signature of 2FL and 3FL becomes ambiguous.

The allowed parameter space of our model can be translated into allowed regions for the GW plateau amplitude $\Omega_{GW}^{\text{plt}} h^2$ and the break frequency f_{dec} (see Supplemental Material II for details). Usually, they are limited from above by the PTA data. However, in our model, they are also bounded from below by the BBN constraint due to the matter-dominated epoch and by the requirement that the spectral break is not due to the particle production from cosmic strings. We find that our scenario implies $10^{-12} \lesssim \Omega_{GW}^{\text{plt}} h^2 \lesssim 10^{-10}$ and $10^{-3} \lesssim f_{\text{dec}}/\text{Hz} \lesssim 10^3$ which we define as the Gravitational Waves windows for Flavored Regimes of Leptogenesis (GWFRL). These ranges, within which a robust GW signature of high-scale leptogenesis is achieved, will be fully explored by planned GW experiments such as LISA, DECIGO and ET. These GWFRL windows also trivially satisfy two important constraints. First, $G\mu < 6.3 \times 10^{-3} g' h(g')$ due to the Hubble friction being always less than m_Φ at $T \simeq T_c$. Second, the ratio of the

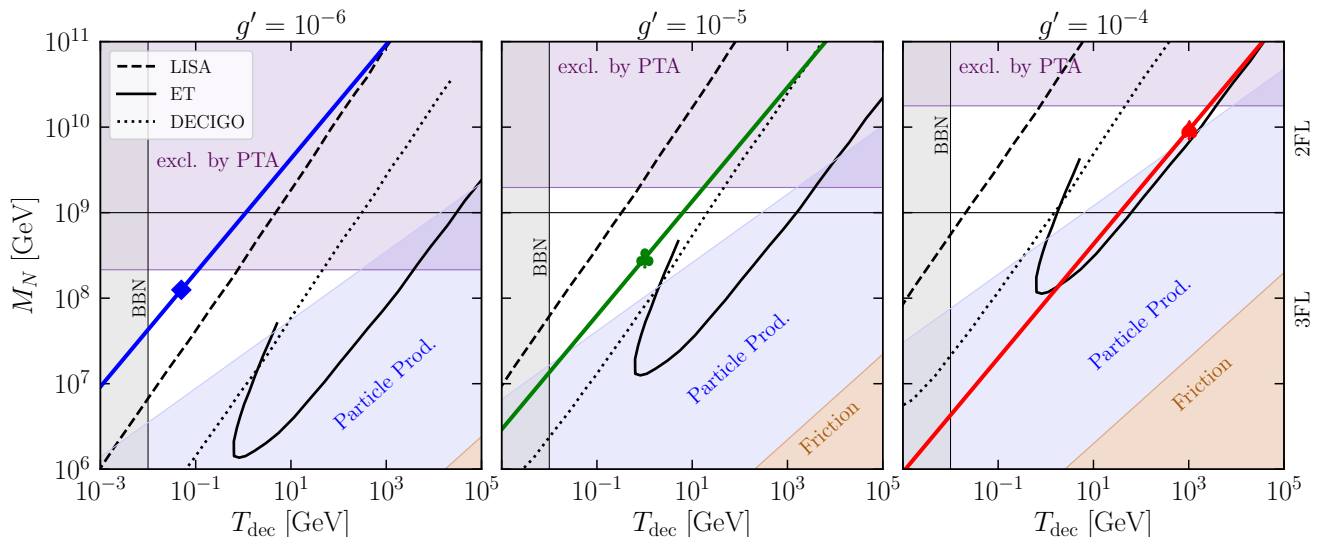


FIG. 2. The white (shaded) regions correspond to the allowed (excluded) model parameter space in the $T_{\text{dec}}-M_N$ plane for $g' = 10^{-6}, 10^{-5}, 10^{-4}$ (left to right). The sensitivity of LISA [36], DECIGO [37] and ET [38] are shown with the black curves. The diagonal colored lines represent the relation Eq. (5) predicted by our model. The symbols correspond to the benchmark cases whose GW spectra are reported in Fig. 1. The black horizontal thin lines mark the separation between the two-flavor (2FL) and the three-flavor (3FL) regimes of thermal leptogenesis.

Φ vacuum energy to the radiation at T_c , which in our case is $\rho_\Phi(T_c)/\rho_R(T_c) = 4.7 \times 10^{-4}g'$, is always smaller than one, thus avoiding a second period of inflation.

There could be possible corrections to the GWFLR windows relaxing some of our assumptions. First, we have considered $\lambda = g'^3$ but a more rigorous parameter space scan could be performed to find a smooth transition of the field and at the same time being consistent with other gauge coupling dependent constraints and a negligible $\Phi \rightarrow Z'Z'$ decays. Second, we have presented our results on GWs for $k = 1$ mode. However, when summing over a large number of modes, the overall amplitude and the spectral break frequency would change slightly. Third, we have assumed $f_N = g'$. Weakening this assumption but being still consistent with Eq. (3) would anyway not modify the overall trend of the parameter space. Indeed, smaller f_N (M_N) would correspond to smaller T_{dec} and therefore smaller f_{dec} , meaning a 3FL regime likely to show up the spectral break at

lower frequencies than the 2FL regime. Summarizing, we point out that the GWFLR windows we have derived in the present paper are quite robust against our assumptions. In conclusions, we demonstrate that different flavor regimes of high-scale leptogenesis can be realistically probed with GW signatures from cosmic strings, thus establishing synergy between low-energy neutrino physics and gravitational waves.

Acknowledgements: We thank Tanmay Vachaspati for useful insight regarding the particle production cut-off. The work of MC, GM, RS, and NS is supported by the research project TASP (Theoretical Astroparticle Physics) funded by the Istituto Nazionale di Fisica Nucleare (INFN). The work of NS is further supported by the research grant number 2022E2J4RK “PANTHEON: Perspectives in Astroparticle and Neutrino THEory with Old and New messengers” under the program PRIN 2022 funded by the Italian Ministero dell’Università e della Ricerca (MUR). The work of SD is supported by the National Natural Science Foundation of China (NNSFC) under grant No. 12150610460.

[1] M. Fukugita and T. Yanagida, *Phys. Lett. B* **174**, 45 (1986).
 [2] P. A. R. Ade *et al.* (Planck), *Astron. Astrophys.* **594**, A13 (2016), arXiv:1502.01589 [astro-ph.CO].
 [3] V. A. Kuzmin, V. A. Rubakov, and M. E. Shaposhnikov, *Phys. Lett. B* **155**, 36 (1985).

[4] S. Davidson, E. Nardi, and Y. Nir, *Phys. Rept.* **466**, 105 (2008), arXiv:0802.2962 [hep-ph].
 [5] W. Buchmuller, P. Di Bari, and M. Plumacher, *Annals Phys.* **315**, 305 (2005), arXiv:hep-ph/0401240.
 [6] A. Abada, S. Davidson, A. Ibarra, F. X. Josse-Michaux, M. Losada, and A. Riotto, *JHEP* **09**, 010 (2006), arXiv:hep-ph/0605281.

- [7] E. Nardi, Y. Nir, E. Roulet, and J. Racker, *JHEP* **01**, 164 (2006), [arXiv:hep-ph/0601084](#).
- [8] S. Blanchet and P. Di Bari, *JCAP* **03**, 018 (2007), [arXiv:hep-ph/0607330](#).
- [9] S. Pascoli, S. T. Petcov, and A. Riotto, *Nucl. Phys. B* **774**, 1 (2007), [arXiv:hep-ph/0611338](#).
- [10] K. Abe *et al.* (T2K), *Phys. Rev. Lett.* **121**, 171802 (2018), [arXiv:1807.07891 \[hep-ex\]](#).
- [11] M. A. Acero *et al.* (NOvA), *Phys. Rev. D* **98**, 032012 (2018), [arXiv:1806.00096 \[hep-ex\]](#).
- [12] J. A. Dror, T. Hiramatsu, K. Kohri, H. Murayama, and G. White, *Phys. Rev. Lett.* **124**, 041804 (2020), [arXiv:1908.03227 \[hep-ph\]](#).
- [13] S. Blasi, V. Brdar, and K. Schmitz, *Phys. Rev. Res.* **2**, 043321 (2020), [arXiv:2004.02889 \[hep-ph\]](#).
- [14] R. Samanta and S. Datta, *JHEP* **05**, 211 (2021), [arXiv:2009.13452 \[hep-ph\]](#).
- [15] S. Datta, A. Ghosal, and R. Samanta, *JCAP* **08**, 021 (2021), [arXiv:2012.14981 \[hep-ph\]](#).
- [16] A. Davidson, *Phys. Rev. D* **20**, 776 (1979).
- [17] R. E. Marshak and R. N. Mohapatra, *Phys. Lett. B* **91**, 222 (1980).
- [18] W. Buchmüller, V. Domcke, K. Kamada, and K. Schmitz, *JCAP* **10**, 003 (2013), [arXiv:1305.3392 \[hep-ph\]](#).
- [19] W. Buchmüller, V. Domcke, H. Murayama, and K. Schmitz, *Phys. Lett. B* **809**, 135764 (2020), [arXiv:1912.03695 \[hep-ph\]](#).
- [20] T. W. B. Kibble, *J. Phys. A* **9**, 1387 (1976).
- [21] M. B. Hindmarsh and T. W. B. Kibble, *Rept. Prog. Phys.* **58**, 477 (1995), [arXiv:hep-ph/9411342](#).
- [22] R. Jeannerot, J. Rocher, and M. Sakellariadou, *Phys. Rev. D* **68**, 103514 (2003), [arXiv:hep-ph/0308134](#).
- [23] A. Vilenkin, *Phys. Lett. B* **107**, 47 (1981).
- [24] T. Vachaspati and A. Vilenkin, *Phys. Rev. D* **31**, 3052 (1985).
- [25] M. Chianese, S. Datta, R. Samanta, and N. Saviano, (2024), [arXiv:2405.00641 \[hep-ph\]](#).
- [26] G. Agazie *et al.* (NANOGrav), *Astrophys. J. Lett.* **951**, L8 (2023), [arXiv:2306.16213 \[astro-ph.HE\]](#).
- [27] J. Antoniadis *et al.* (EPTA, InPTA:), *Astron. Astrophys.* **678**, A50 (2023), [arXiv:2306.16214 \[astro-ph.HE\]](#).
- [28] D. J. Reardon *et al.*, *Astrophys. J. Lett.* **951**, L6 (2023), [arXiv:2306.16215 \[astro-ph.HE\]](#).
- [29] H. Xu *et al.*, *Res. Astron. Astrophys.* **23**, 075024 (2023), [arXiv:2306.16216 \[astro-ph.HE\]](#).
- [30] J. Antoniadis *et al.* (EPTA), (2023), [arXiv:2306.16227 \[astro-ph.CO\]](#).
- [31] A. Afzal *et al.* (NANOGrav), *Astrophys. J. Lett.* **951**, L11 (2023), [arXiv:2306.16219 \[astro-ph.HE\]](#).
- [32] D. Matsunami, L. Pogosian, A. Saurabh, and T. Vachaspati, *Phys. Rev. Lett.* **122**, 201301 (2019), [arXiv:1903.05102 \[hep-ph\]](#).
- [33] P. Auclair, D. A. Steer, and T. Vachaspati, *Phys. Rev. D* **101**, 083511 (2020), [arXiv:1911.12066 \[hep-ph\]](#).
- [34] R. H. Cyburt, B. D. Fields, K. A. Olive, and T.-H. Yeh, *Rev. Mod. Phys.* **88**, 015004 (2016), [arXiv:1505.01076 \[astro-ph.CO\]](#).
- [35] T. Hasegawa, N. Hiroshima, K. Kohri, R. S. L. Hansen, T. Tram, and S. Hannestad, *JCAP* **12**, 012 (2019), [arXiv:1908.10189 \[hep-ph\]](#).
- [36] P. Amaro-Seoane *et al.* (LISA), (2017), [arXiv:1702.00786 \[astro-ph.IM\]](#).
- [37] S. Kawamura *et al.*, *Class. Quant. Grav.* **23**, S125 (2006).
- [38] B. Sathyaprakash *et al.*, *Class. Quant. Grav.* **29**, 124013 (2012), [Erratum: *Class. Quant. Grav.* **30**, 079501 (2013)], [arXiv:1206.0331 \[gr-qc\]](#).
- [39] A. D. Linde, *Rept. Prog. Phys.* **42**, 389 (1979).
- [40] T. W. B. Kibble, *Phys. Rept.* **67**, 183 (1980).
- [41] S. Datta and R. Samanta, *Phys. Rev. D* **108**, L091706 (2023), [arXiv:2307.00646 \[hep-ph\]](#).
- [42] E. Masso, F. Rota, and G. Zsembinszki, *Phys. Rev. D* **72**, 084007 (2005), [arXiv:astro-ph/0501381](#).
- [43] S. Datta and R. Samanta, *JHEP* **11**, 159 (2022), [arXiv:2208.09949 \[hep-ph\]](#).
- [44] C. Gross, O. Lebedev, and M. Zatta, *Phys. Lett. B* **753**, 178 (2016), [arXiv:1506.05106 \[hep-ph\]](#).
- [45] K. Enqvist, M. Karčiauskas, O. Lebedev, S. Rusak, and M. Zatta, *JCAP* **11**, 025 (2016), [arXiv:1608.08848 \[hep-ph\]](#).
- [46] T. Han and X. Wang, *JHEP* **10**, 036 (2017), [arXiv:1704.00790 \[hep-ph\]](#).
- [47] C. T. Hill, H. M. Hodges, and M. S. Turner, *Phys. Rev. D* **37**, 263 (1988).
- [48] J. J. Blanco-Pillado, K. D. Olum, and B. Shlaer, *Phys. Rev. D* **89**, 023512 (2014), [arXiv:1309.6637 \[astro-ph.CO\]](#).
- [49] J. J. Blanco-Pillado and K. D. Olum, *Phys. Rev. D* **96**, 104046 (2017), [arXiv:1709.02693 \[astro-ph.CO\]](#).
- [50] C. J. A. P. Martins and E. P. S. Shellard, *Phys. Rev. D* **54**, 2535 (1996), [arXiv:hep-ph/9602271](#).
- [51] C. J. A. P. Martins and E. P. S. Shellard, *Phys. Rev. D* **65**, 043514 (2002), [arXiv:hep-ph/0003298](#).
- [52] L. Sousa and P. P. Avelino, *Phys. Rev. D* **88**, 023516 (2013), [arXiv:1304.2445 \[astro-ph.CO\]](#).
- [53] P. Auclair *et al.*, *JCAP* **04**, 034 (2020), [arXiv:1909.00819 \[astro-ph.CO\]](#).
- [54] T. Damour and A. Vilenkin, *Phys. Rev. D* **64**, 064008 (2001), [arXiv:gr-qc/0104026](#).
- [55] A. Vilenkin, *Phys. Rev. D* **43**, 1060 (1991).
- [56] L. Sousa, P. P. Avelino, and G. S. F. Guedes, *Phys. Rev. D* **101**, 103508 (2020), [arXiv:2002.01079 \[astro-ph.CO\]](#).
- [57] Y. Cui, M. Lewicki, D. E. Morrissey, and J. D. Wells, *JHEP* **01**, 081 (2019), [arXiv:1808.08968 \[hep-ph\]](#).

Supplemental Material for Probing flavored regimes of leptogenesis with gravitational waves from cosmic strings

Marco Chianese, Satyabrata Datta, Gennaro Miele, Rome Samanta, and Ninetta Saviano

The Supplemental Material is organized as follows. In Sec. I, we discuss the evolution of the radiation and the scalar field energy densities, and the produced entropy with the inverse of temperature. We derive the analytical expressions for the decay temperature T_{dec} and the amount κ of the produced entropy which match the numerical results well. In Sec. II, we detail the constraints leading to the Gravitational Waves window for Flavored Regimes of Leptogenesis (GWFRL).

I. SCALAR FIELD EVOLUTION AND ENTROPY PRODUCTION

The scalar field Φ with initial vacuum energy $\rho_{\Phi}(T_c) \simeq \lambda v_{\Phi}^4/4$ dominates the energy density for a period, and injects entropy as it decays. We account for this effect by solving the following Friedmann equations:

$$\frac{d\rho_R}{dt} + 4\mathcal{H}\rho_R = \Gamma_{\Phi}^{HH}\rho_{\Phi}, \quad \frac{d\rho_{\Phi}}{dt} + 3\mathcal{H}\rho_{\Phi} = -\Gamma_{\Phi}^{HH}\rho_{\Phi}, \quad \frac{ds}{dt} + 3\mathcal{H}s = \Gamma_{\Phi}^{hh}\frac{\rho_{\Phi}}{T}, \quad (\text{S1})$$

and upon recasting them as

$$\frac{d\rho_R}{dz} + \frac{4}{z}\rho_R = 0, \quad \frac{d\rho_{\Phi}}{dz} + \frac{3}{z}\frac{\mathcal{H}}{\tilde{\mathcal{H}}}\rho_{\Phi} + \Gamma_{\Phi}^{HH}\frac{1}{z\tilde{\mathcal{H}}}\rho_{\Phi} = 0, \quad (\text{S2})$$

where ρ_R and ρ_{Φ} are the energy densities of radiona and the scalar field as a function of $z = T_c/T$, \mathcal{H} is the Hubble parameter, s is the entropy density of the thermal bath, and the temperature-time relation has been derived from the third of Eq. (S1) as

$$\frac{1}{T} \frac{dT}{dt} = - \left(\mathcal{H} + \frac{1}{3g_{*s}(T)} \frac{dg_{*s}(T)}{dt} - \Gamma_{\Phi}^{HH} \frac{\rho_{\Phi}}{4\rho_R} \right) = -\tilde{\mathcal{H}}, \quad (\text{S3})$$

with a and g_{*s} being the scale factor and the number of degree of freedom, respectively. The production of entropy from the Φ decays is computed by solving

$$\frac{da}{dz} = \left(1 + \Gamma_{\Phi}^{hh} \frac{\rho_{\Phi}}{4\rho_R \tilde{\mathcal{H}}} \right) \frac{a}{z}, \quad (\text{S4})$$

and computing the ratio of $\tilde{S} \sim a^3/z^3$ after and before the scalar field decay. The amount of entropy production $\kappa = \tilde{S}_{\text{after}}/\tilde{S}_{\text{before}}$ can be analytically quantified as

$$\kappa \simeq \left[\frac{\rho_R(T_c)}{\rho_{\Phi}(T_c)} \frac{T_{\text{dec}}}{T_c} \right]^{-1} \simeq \frac{\rho_{\Phi}(T_c)}{3^{1/4} \left(\frac{30}{\pi^2 g_*} \right)^{-3/4} T_c^3 \sqrt{\Gamma_{\Phi}^{HH} \tilde{M}_{\text{Pl}}}} \simeq 140 \left(\frac{g'}{10^{-3}} \right)^{-1/4} \left(\frac{M_N}{10^9 \text{ GeV}} \right)^{-1/2}, \quad (\text{S5})$$

by considering $\Gamma_{\Phi}^{HH} \simeq \mathcal{H}$ which gives the decay temperature T_{dec}

$$T_{\text{dec}} \simeq \left(\frac{90}{\pi^2 g_*} \right)^{1/4} \sqrt{\Gamma_{\Phi}^{HH} \tilde{M}_{\text{Pl}}} \simeq 6.35 \left(\frac{g'}{10^{-5}} \right)^{3/4} \left(\frac{M_N}{10^9 \text{ GeV}} \right)^{3/2} \text{ GeV}, \quad (\text{S6})$$

with $\tilde{M}_{\text{Pl}} = 2.4 \times 10^{18}$ GeV being the reduced Planck constant, and $g_* \simeq 106.75$ is the effective degrees of freedom that contribute to the radiation. The evolution of the radiation, the scalar field normalized energy densities $\Omega_i = \rho_i/\rho_{\text{tot}}$, and the entropy production factor κ corresponding to the benchmarks discussed in the main text are shown in Fig. S1.

II. GRAVITATIONAL WAVES WINDOW FOR FLAVORED REGIMES OF LEPTOGENESIS (GWFRL)

We here detail the upper and lower bounds on the the GW plateau amplitude $\Omega_{\text{GW}}^{\text{plt}} h^2$ and the break frequency f_{dec} which allow us to define the GWFRL windows reported in Fig. S2. These regions are bounded from below by either the BBN or the particle production constraint, and from above by the PTA observations. The lower bounds

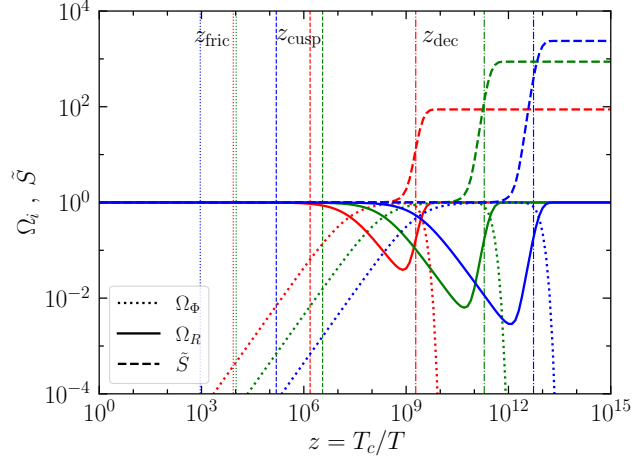


FIG. S1. Evolution of the radiation and the scalar field normalized energy densities $\Omega_i = \rho_i/\rho_{\text{tot}}$, and the entropy production factor κ corresponding to the benchmarks discussed in the main text. Because only the ratio of entropies before and after the Φ decay matters, we set $\kappa(T_C) = 1$. The vertical lines represent the cut-off temperatures $T_{\text{fric}} \gg T_{\text{fric}} \gg T_{\text{dec}}$, implying that the fall in the GW spectra occurs due to the M_N -dependent matter domination.

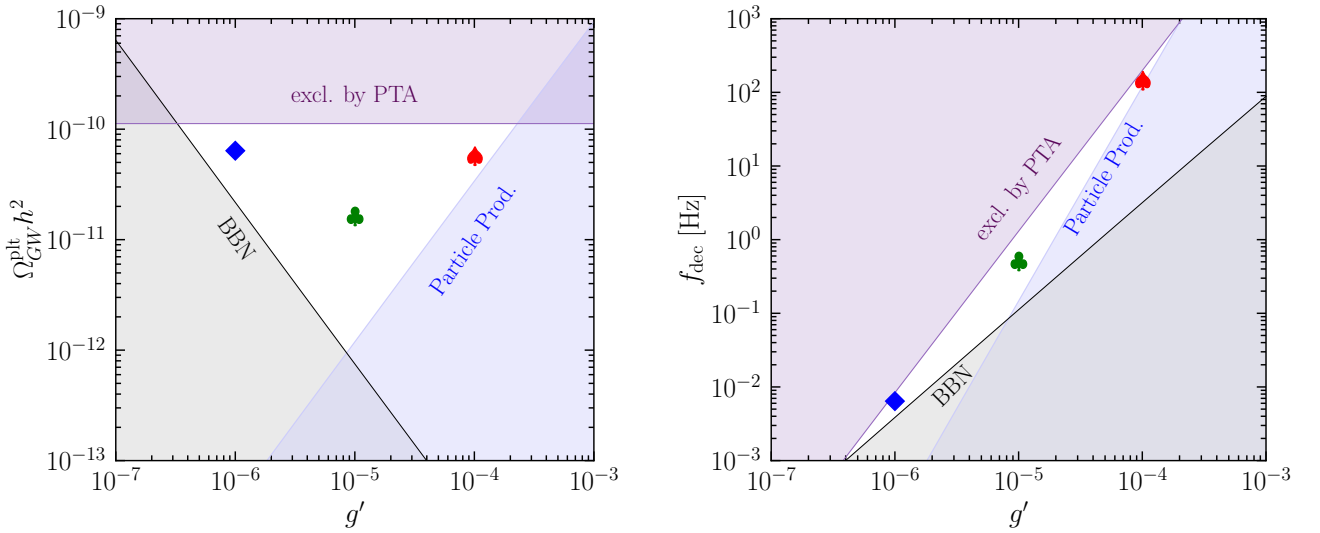


FIG. S2. The white regions are allowed windows for the GW plateau amplitude (left) and the spectral break frequencies (right), referred to as Gravitational Waves Window for Flavored Regimes of Leptogenesis (GWFR) in the main text. These windows are derived from the spectral features of GWs radiated from the fundamental mode oscillation of cosmic string loops. The symbols correspond to the benchmark cases discussed in the main text.

on the GW amplitude (from Eq. (9)) come from the lower bound on $G\mu$ imposed by BBN and particle production from cosmic strings, which read

$$(G\mu)^{\text{BBN}} \gtrsim 3.8 \times 10^{-14} \left(\frac{g'}{10^{-5}} \right)^{-3} h(g'), \quad (\text{S7})$$

$$(G\mu)^c \gtrsim 6.4 \times 10^{-16} \left(\frac{g'}{10^{-5}} \right)^3 h(g')^{-1}. \quad (\text{S8})$$

Similarly, the lower bounds on the spectral break frequency are derived as

$$f_{\text{dec}}^{\text{BBN}} \gtrsim 3.2 \times 10^{-2} \left(\frac{g'}{10^{-5}} \right)^{3/2} h(g')^{-1/2} \text{ Hz}, \quad (\text{S9})$$

$$f_{\text{dec}}^c \gtrsim 1.2 \times 10^{-2} \left(\frac{g'}{10^{-5}} \right)^3 h(g')^{-1} \text{ Hz}. \quad (\text{S10})$$

The upper bound on the plateau amplitude is given by

$$(G\mu)^{\text{PTA}} \lesssim 7.0 \times 10^{-11}. \quad (\text{S11})$$

while for $f_{\text{dec}}^{\text{PTA}}$ we have

$$f_{\text{dec}}^{\text{PTA}} \lesssim 2.0 \times 10^{-1} \left(\frac{g'}{10^{-5}} \right)^{9/4} h(g')^{-3/4} \text{ Hz}. \quad (\text{S12})$$